nature genetics

Dynamics of the p53-Mdm2 feedback loop in individual cells

Galit Lahav[1], Nitzan Rosenfeld[1], Alex Sigal[1], Naama Geva-Zatorsky[1], Arnold J Levine[2], Michael B Elowitz[3] & Uri Alon[1]

The tumor suppressor p53, one of the most intensely investigated proteins[1–5], is usually studied by experiments that are averaged over cell populations, potentially masking the dynamic behavior in individual cells. We present a system for following, in individual living cells, the dynamics of p53 and its negative regulator Mdm2 (refs. 1, 4–7): this system uses functional p53-CFP and Mdm2-YFP fusion proteins and time-lapse fluorescence microscopy. We found that p53 was expressed in a series of discrete pulses after DNA damage. Genetically identical cells had different numbers of pulses: zero, one, two or more. The mean height and duration of each pulse were fixed and did not depend on the amount of DNA damage. The mean number of pulses, however, increased with DNA damage. This approach can be used to study other signaling systems and suggests that the p53-Mdm2 feedback loop generates a 'digital' clock that releases well-timed quanta of p53 until damage is repaired or the cell dies.

A common network motif[8] across organisms is a negative feedback loop composed of one transcription arm and one protein-interaction arm (**Fig. 1a**). Here we chose one of the best-studied examples in human cells, in which the tumor suppressor p53 transcriptionally activates Mdm2, which in turn targets p53 for degradation (**Fig. 1b**)[1–5]. After stresses such as DNA damage, a decrease in the activity of Mdm2
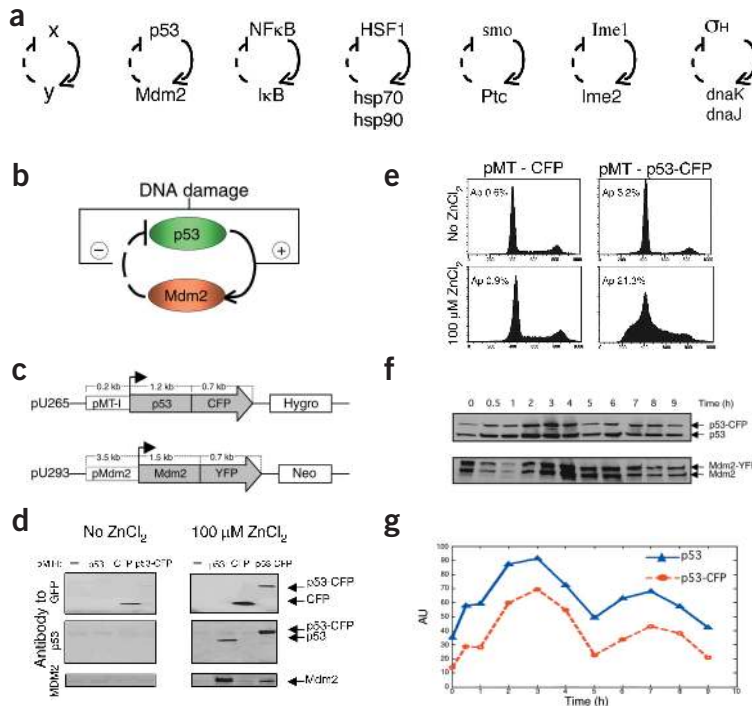
Figure 1 The p53-Mdm2 system and the fluorescent protein fusion system. (**a**) Examples of the negative feedback loop motif with one transcription arm and one protein-protein interaction arm in diverse systems in mammals[10,27], fruit flies[28], yeast[29] and bacteria[30]. (**b**) The p53-Mdm2 negative feedback loop: after DNA damage, p53 is activated as a transcription factor and Mdm2-p53 interaction decreases[1–7]. (**c**) p53-CFP and Mdm2-YFP constructs. (**d**) Immunoblots with antibodies to GFP (and CFP), p53 and Mdm2, with or without 6-h zinc induction, on H1299 cells stably transfected with p53, CFP or p53-CFP expressed under pMT-I. (**e**) Cell-cycle distribution by flow cytometry of H1299 cells expressing p53-CFP or CFP, with or without 48-h zinc induction, stained with 25 μg ml−1 of propidium iodide. Ap is the percentage of cells in the sub-G1 region, representing the apoptotic subpopulation. (**f**) Immunoblot kinetics of p53 and p53-CFP (antibody to p53) and Mdm2 and Mdm2-YFP (antibody to Mdm2) at the indicated times (in h) after 5-Gy of γ-irradiation in a MCF7 cell clone stably transfected with pU265 and pU293. (**g**) Quantification of p53. AU, arbitrary units.

and in the interaction between Mdm2 and p53 leads to p53 stabilization[1,4–7]. The increase in p53 protein levels and in the transcription activity of p53 lead, in turn, to increased production of Mdm2 (**Fig. 1b**)[1–6]. Analysis of cell populations with the use of immunoblots showed that p53 and Mdm2 undergo damped oscillations after strong, but not after weak, DNA damage[9]. Damped oscillations at the population level were also observed in the NF-κB system[10], which has a similar feedback loop structure (**Fig. 1a**). Generally, in these systems, the behavior observed in immunoblots is graded: the stronger the stimulus, the stronger the amplitude of the average response.

We sought to observe p53 and Mdm2 behavior at the level of individual cells. For this purpose, we generated stable cell lines that expressed p53 and Mdm2 fused to fluorescent proteins. p53 was fused to cyan fluorescent protein (CFP) under a zinc-inducible promoter[11], and Mdm2 was fused to yellow fluorescent protein (YFP) under the human Mdm2 native promoter (**Fig. 1c**). We established stable cell lines in p53 wild-type (MCF7; ref. 11) and p53-null (H1299; ref. 12) cells. These cell lines expressed full-length p53-CFP upon zinc induction (**Fig. 1d**). p53-CFP

activated transcription of endogenous Mdm2 (**Fig. 1d**), indicating that the fusion protein functions as a transcription factor. The p53-CFP fusion protein was also functional in causing apoptosis after zinc induction in a clone, in contrast to the CFP control (**Fig. 1e**). Immunoblots on cell populations showed that both endogenous p53 and exogenous p53-CFP undergo nearly identical damped oscillation after γ-irradiation (**Fig. 1f,g**). Similarly, immunoblots showed that after DNA damage Mdm2-YFP showed kinetic behavior that was almost identical to that of endogenous Mdm2, including an early decrease at 0.5–1 h (**Fig. 1f**)[13]. Thus, the p53-CFP and Mdm2-YFP system can be used to follow the dynamics of the endogenous proteins.

Immunoblots have limited resolution because they report averages of cell populations. To observe the protein levels in individual cells, we took time-lapse fluorescence microscopy movies of a cell line clone that was expressing both p53-CFP and Mdm2-YFP after γ-irradiation at a 20 min resolution during 16 h of growth. γ-irradiation causes double-stranded DNA breaks and induces p53 activation[1,7,14]. We measured total CFP and YFP fluorescence in the nuclei of over 200
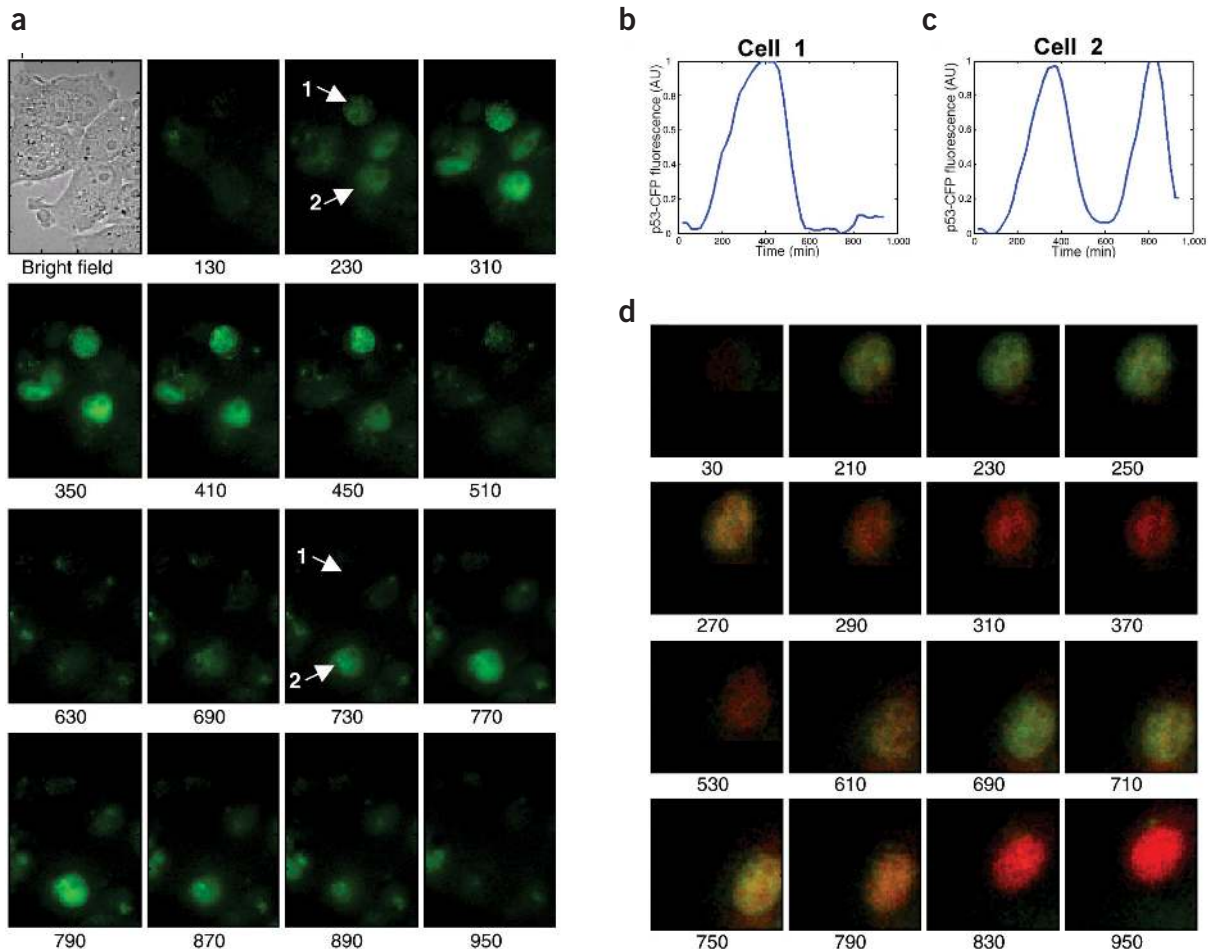
Figure 2 Dynamics of p53-CFP. (**a**) p53-CFP (green) in clonal MCF7+pU265+pU293 cells after 5-Gy γ-irradiation. Time (in min) after irradiation is shown below images. (**b,c**) p53-CFP levels (total CFP fluorescence in nuclei) from cells 1 and 2 (indicated by arrows in **a**). (**d**) Dynamics of p53-CFP (green) and Mdm2-YFP (red) in a cell that shows two pulses. Time (in min) after irradiation is shown below images. (**e**) p53-CFP (green) and Mdm2-YFP (red) levels in the nucleus of the cell in **d**. AU, arbitrary units.
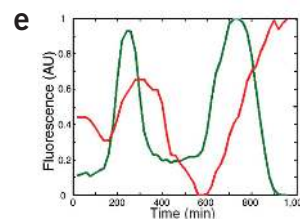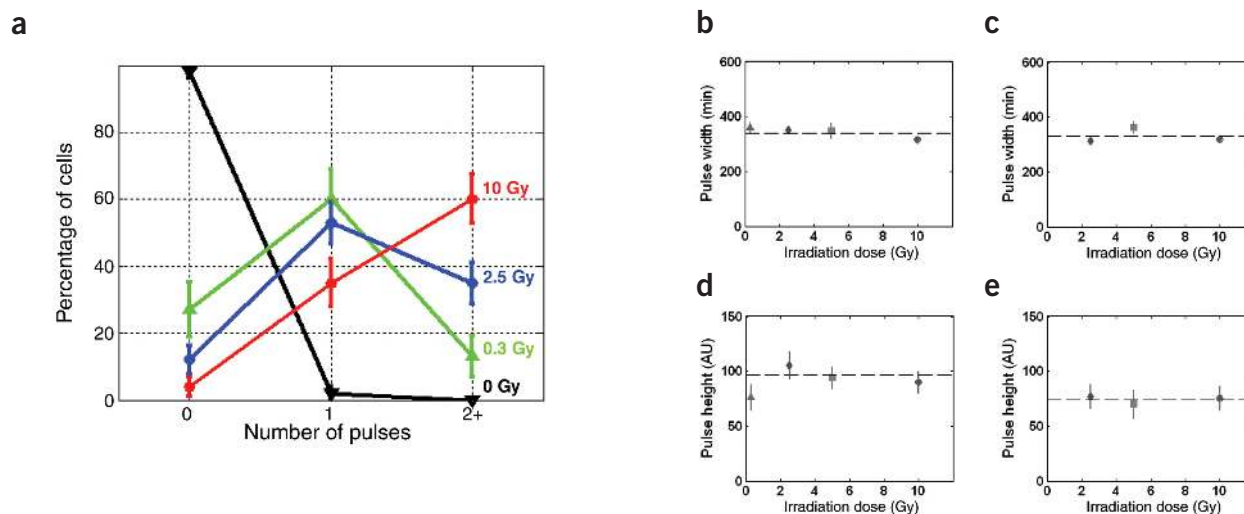
Figure 3 Digital behavior in p53 oscillations. (**a**) Fraction of cells with zero, one, two or more pulses as a function of γ-irradiation dose. The solid lines connecting the points were drawn to aid interpretation. Irradiation dose dependence of (**b**) first pulse width, (**c**) second pulse width, (**d**) first pulse height and (**e**) second pulse height. Mean ± s.e.m. data for 20–100 cells are shown. AU, arbitrary units.

different cells. The movies showed p53-CFP oscillations occurring in individual cells (**Fig. 2a**). A control CFP movie showed constant CFP levels rather than oscillations over time (data not shown). Different cells from the same clone in the same field of view showed different numbers of oscillations (**Fig. 2a–c**), with cells showing either zero, one (**Fig. 2b**) or two (**Fig. 2c**) pulses (some cells began a third pulse towards the end of the movies). The width of each pulse was 350 ± 160 min (mean ± s.d.). The timing of the first pulse maximum was rather variable, 360 ± 240 min after damage, but the time between the maxima of two consecutive pulses was more precise, 440 ± 100 min (mean ± s.d.). Pulse heights varied by approximately threefold between cells. The heights of different pulses in the same cell also varied by about threefold; the mean height of the second pulse, however, was approximately equal to that of the first pulse. Mdm2-YFP also showed oscillations, at a ~100 min delay relative to the p53-CFP oscillations. The number of Mdm2 pulses was equal to the number of p53 pulses in almost all cells. **Figure 2d** shows a cell with two pulses (green is p53-CFP, red is Mdm2-YFP and yellow is colocalization of CFP and YFP). In each pulse, p53-CFP first appeared in the nucleus, followed, after a delay, by Mdm2-YFP (**Fig. 2d,e**). Nuclear p53-CFP levels then decreased, and finally nuclear Mdm2-YFP levels declined (**Fig. 2d**). A second pulse then occurred, peaking at ~700 min. Synchronized populations showed similar behavior (data not shown), which suggests that the variability between cells was not due to differences in cell-cycle stages[15]. Averages of the individual cell data showed damped oscillations with a second peak that was smaller and broader than the first peak; this was similar to the immunoblot data (**Fig. 1g**), which resulted from averaging between cells with different numbers of pulses.

The response to different doses of γ-irradiation differed from the behavior predicted by immunoblots. The fraction of cells with zero pulses decreased with irradiation dose, whereas the fraction of cells with two or more pulses increased with irradiation dose (**Fig. 3a**). Thus, cells tend to show more pulses as damage increases. The mean height and width of each pulse, however, was constant and did not depend on irradiation dose (**Fig. 3b–e**). In contrast, at the population level, the average amplitude of the response appeared to increase with DNA damage, due to the averaging of cell populations with different numbers of pulses.

Our findings suggest that the behavior of the p53-Mdm2 feedback loop can be thought of as 'digital', as opposed to 'analog'. In an analog system, the stronger the input signal, the higher and broader the output (**Fig. 4a**). In contrast, in the p53-Mdm2 system, we found that the number of pulses, but not the size or shape of each pulse, depended on the level of the input signal (**Fig. 4b**). Pulsatile release also has an important role in other biological systems, such as cyclic turnover on promoters and hormone production[16,17]. Most hormones are secreted in a pulsatile rather than continuous manner, and the temporal pattern of a hormone is often as important as its concentration[17]. Digital pulses are distinct from switch-like or all-or-nothing responses[18] (which usually consist of a single step-like response) and from analog (graded) pulses (whose amplitude continuously increases with input signal)[9,19].

What is the mechanism for digital oscillations in this system? Digital, undamped oscillatory behavior is a challenge to modelers
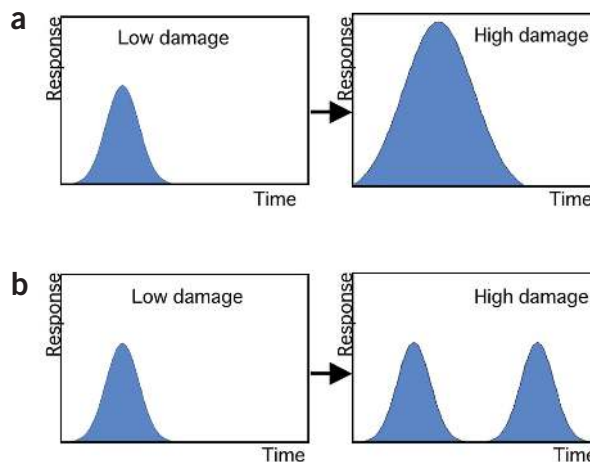
Figure 4 Analog and digital behaviors. (**a**) The response of analog systems continuously grows with increasing signal. (**b**) Digital systems show an increased number of pulses with increasing signal, but the pulse size and shape do not depend on the signal strength.

because the simplest theoretical models of this negative feedback loop show damped, analog oscillations[9,19]. Mechanisms such as positive feedback on p53 (refs. 20,21) may enhance undamped oscillatory behavior[22,23]. Digital behavior may require a damage checkpoint, which functions when p53 levels are low, inciting the next pulse only if damage is still present. Future studies could determine whether different numbers of pulses convey different 'meanings' to the cell in terms of expression of downstream genes. It is possible that the digital behavior of the p53-Mdm2 system evolved to give reasonably defined quanta of repair enzymes in response to stress, reducing the risk of having too much p53 and leading to cell death.

Finally, we suggest three criteria that can be generally used to define digital oscillations in biological systems: (i) output is in discrete pulses or quanta; (ii) the fraction of cells with a given number of pulses depends on the input signal strength; and (iii) the mean size and shape of each pulse does not depend on the input signal strength (**Fig. 4**). Digital clocks are well known in the context of electronic designs, where they reduce noise and provide robustness against component tolerances. It will be important to determine whether additional cell-signaling systems, such as those with the negative feedback motif (**Fig. 1a**), also show digital oscillations.

METHODS

Plasmids and cells. To generate pU265, we subcloned ECFP from pECFP-C1 (Clontech) after the last codon of cDNA encoding p53 under the rat metallothionein-1 promoter (MTΔ156; ref. 24). To construct pU293, we cloned the hMDM2 promoter by PCR with the use of genomic DNA as a template, generating a 3.5-kb fragment upstream of the ATG site in exon 3, which includes P1 and P2 (ref. 25). An XhoI site was inserted before exon 3. We subcloned this promoter into pEYFP-1 (Clontech); hMDM2 cDNA from pCMV-hMDM2 was subcloned before the first codon of EYFP. We maintained human non-small lung carcinoma H1299 cells (p53-null) and human breast cancer epithelial MCF-7 cells (p53 wild-type) at 37 °C in RPMI medium supplemented with 10% fetal calf serum and 2 mM glutamine. Transfection used standard procedures (Fugene 6 transfection reagents, Boehringer Mannheim), and we selected stable clones with flow cytometry for cells expressing CFP and YFP.

Immunoblots. We collected protein samples and normalized the lysates by Bradford assay. We separated equal amounts of protein by electrophoresis on 4−15% gradient polyacrylamide SDS gel (BioRad). We detected CFP and p53-CFP proteins with B-2 monoclonal antibody (mAb; Santa Cruz Biotechnology). We detected p53 and p53-CFP proteins with DO-1 mAb (Santa Cruz Biotechnology). We detected Mdm2 with SMP-14 mAb (Santa Cruz Biotechnology). Gel quantification used Scion imaging.

Time-lapse microscopy. We grew cells in a 96-well optical plate (Nunc) in a HEPES medium containing 50 μg ml^{-1} of hygromycin and 400 μg ml^{-1} of neomycin; the medium lacked riboflavin and phenol red. No zinc was added and so p53-CFP expression was driven by basal expression from the pMT-1 promoter. We then exposed cells to γ-irradiation (^{60}Co, 2.2 Gy min^{-1}). Double-stranded DNA breaks (DSBs) are linear in γ-irradiation doses and cause on average ~30 DSBs per Gy per cell[26]. We viewed cells with an inverted fluorescence microscope (Olympus IX70). CFP filter set: excitation 436 nm/20 nm, dichroic beam splitter 455 nm and emission 480 nm/40 nm. YFP filter set: excitation 500 nm/20 nm, a dichroic beam splitter 515 nm and emission 535 nm/30 nm. We captured images with a cooled back-illuminated CCD camera (Photometrics Quantix 57). Relative fluorescence analysis and background subtraction was done with the use of custom-written Matlab software.

1. Vogelstein, B., Lane, D. & Levine, A.J. Surfing the p53 network. *Nature* **408**, 307–310 (2000).
2. Michael, D. & Oren, M. The p53-Mdm2 module and the ubiquitin system. *Semin. Cancer Biol.* **13**, 49–58 (2003).
3. Piette, J., Neel, H. & Marechal, V. Mdm2: keeping p53 under control. *Oncogene* **15**, 1001–1010 (1997).
4. Prives, C. Signaling to p53: breaking the MDM2-p53 circuit. *Cell* **95**, 5–8 (1998).
5. Momand, J., Wu, H.H. & Dasgupta, G. MDM2-master regulator of the p53 tumor suppressor protein. *Gene* **242**, 15–29 (2000).
6. Larkin, N.D. & Jackson, S.P. Regulation of p53 in response to DNA damage. *Oncogene* **18**, 7644–7655 (1999).
7. Ryan, K.M., Phillips, A.C. & Vousden, K.H. Regulation and function of the p53 tumor suppressor protein. *Curr. Opin. Cell Biol.* **13**, 332–337 (2001).
8. Shen-Orr, S., Milo, R., Mangan, S. & Alon, U. Network motifs in the transcriptional regulation network of *Escherichia coli*. *Nat. Genet.* **31**, 64–68 (2002).
9. Lev Bar-Or, R. *et al.* Generation of Oscillation by the p53-Mdm2 feedback loop: a theoretical and experimental study. *Proc. Natl. Acad. Sci. USA* **97**, 11250–11255 (2000).
10. Hoffmann, A., Levchenko, A., Scott, M.L. & Baltimore, D. The IκB-NF-κB signaling module: Temporal control and selective gene activation. *Science* **298**, 1241–1245 (2002).
11. Vojtesek, B. & Lane, D.P. Regulation of p53 protein expression in human breast cancer cell lines. *J. Cell. Sci.* **105**, 607–612 (1993).
12. Mitsudomi, T. *et al.* p53 gene mutations in non-small-cell lung cancer cell lines and their correlation with the presence of ras mutations and clinical features. *Oncogene* **7**, 171–180 (1992).
13. Zhang, T. & Prives, C. Cyclin a-CDK phosphorylation regulates MDM2 protein interactions. *J. Biol. Chem.* **276**, 29702–29710 (2001).
14. Khosravi, R. *et al.* Rapid ATP-dependent phosphorylation of MDM2 precedes p53 accumulation in response to DNA damage. *Proc. Natl. Acad. Sci. USA* **96**, 14973–14977 (1999).
15. Offer, H. *et al.* p53 modulates base excision repair activity in a cell cycle-specific manner after genotoxic stress. *Cancer Res.* **61**, 88–96 (2001).
16. Reid, G. *et al.* Cyclic, proteasome-mediated turnover of unliganded and liganded ERa on responsive promoters is an integral feature of estrogen signaling. *Mol. Cell* **11**, 605–707 (2003).
17. Goldbeter, A. Computational approaches to cellular rhythms. *Nature* **420**, 238–245 (2002).
18. Ferrell, J.E. Jr. & Machleder, E.M. The biochemical basis of an all-or-none cell fate switch in *Xenopus* oocytes. *Science* **280**, 895–898 (1998).
19. Mihalas, G.I., Simon, Z., Balea, G. & Popa, E. Possible oscillatory behavior in p53-Mdm2 interaction computer simulation. *J. Biol. Syst.* **8**, 21–29 (2000).
20. Mayo, L.D., Dixon, J.E., Durden, D.L., Tonks, N.K. & Donner, D.B. PTEN protects p53 from Mdm2 and sensitizes cancer cells to chemotherapy. *J. Biol. Chem.* **277**, 5484–5489 (2002).
21. Deguin-Chambon, V., Vacher, M., Jullien, M., May, E. & Bourdon, J.C. Direct transactivation of c-Ha-Ras gene by p53: evidence for its involvement in p53 transactivation activity and p53-mediated apoptosis. *Oncogene* **19**, 5831–5841 (2000).
22. Pomerening, J.R., Sontag, E.D. & Ferrell, J.E. Jr. Building a cell cycle oscillator: hysteresis and bistability in the activation of Cdc2. *Nat. Cell Biol.* **5**, 346–351 (2003).
23. Tyson, J.J., Chen, K.C. & Novak, B. Sniffers, buzzers, toggles and blinkers: dynamics of regulatory and signaling pathways in the cell. *Curr. Opin. Cell Biol.* **15**, 221–231 (2003).
24. Andersen, R.D. *et al.* Metal dependent binding of a factor in vivo to the metal-responsive elements of the metallothionein 1 gene promoter. *Mol. Cell Biol.* **7**, 3574–3581 (1987).
25. Oliner, J.D., Kinzler, K.W., Meltzer, P.S., George, D.L. & Vogelstein, B. Amplification of a gene encoding a p53-associated protein in human sarcomas. *Nature* **358**, 80–83 (1992).
26. Bonner, W.M. Low-dose rediation: thresholds, bystander effects, and adaptive responses. *Proc. Natl. Acad. Sci. USA* **100**, 4973–4975 (2003).
27. Santoro, M.G. Heat shock factors and the control of the stress response. *Biochem. Pharmacol.* **59**, 55–63 (2000).
28. Alcedo, J., Zou, Y. & Noll, M. Posttranscriptional regulation of Smoothened is part of a self-correcting mechanism in the Hedgehog signaling system. *Mol. Cell* **6**, 457–465 (2000).
29. Guttman-Raviv, N., Matin, S. & Kassir, Y. Ime2, a meiosis-specific kinase in yeast, is required for destabilization of its transcriptional activator, Ime1. *Mol. Cell. Biol.* **22**, 2047–2056 (2002).
30. Straus, D., Walter, W. & Gross, C.A. DnaK, DnaJ, and GrpE heat shock proteins negatively regulate heat shock gene expression by controlling the synthesis and stability of sigma 32. *Genes Dev.* **4**, 2202–2209 (1990).